Directing differentiation of human induced pluripotent stem cells toward androgen-producing Leydig cells rather than adrenal cells

Lu Li[a], Yuchang Li[a], Chantal Sottas[a], Martine Culty[a], Jinjiang Fan[b,c], Yiman Hu[a], Garett Cheung[a], Héctor E. Chemes[d], and Vassilios Papadopoulos[a,b,c,1]

[a]Department of Pharmacology and Pharmaceutical Sciences, School of Pharmacy, University of Southern California, Los Angeles, CA 90089; [b]The Research Institute of the McGill University Health Centre, Montreal, QC H4A 3J1, Canada; [c]Department of Medicine, McGill University, Montreal, QC H4A 3J1, Canada; and [d]Centro de Investigaciones Endocrinológicas (CEDIE–Consejo Nacional de Investigaciones Científicas y Técnicas), Hospital de Niños R. Gutiérrez, Buenos Aires C1425EFD, Argentina

Edited by R. Michael Roberts, University of Missouri, Columbia, MO, and approved September 17, 2019 (received for review May 13, 2019)

Reduced serum testosterone (T), or hypogonadism, affects millions of men and is associated with many pathologies, including infertility, cardiovascular diseases, metabolic syndrome, and decreased libido and sexual function. Administering T-replacement therapy (TRT) reverses many of the symptoms associated with low T levels. However, TRT is linked to side effects such as infertility and increased risk of prostate cancer and cardiovascular diseases. Thus, there is a need to obtain T-producing cells that could be used to treat hypogonadism via transplantation and reestablishment of T-producing cell lineages in the body. T is synthesized by Leydig cells (LCs), proposed to derive from mesenchymal cells of mesonephric origin. Although mesenchymal cells have been successfully induced into LCs, the limited source and possible trauma to donors hinders their application to clinical therapies. Alternatively, human induced pluripotent stem cells (hiPSCs), which are expandable in culture and have the potential to differentiate into all somatic cell types, have become the emerging source of autologous cell therapies. We have successfully induced the differentiation of hiPSCs into either human Leydig-like (hLLCs) or adrenal-like cells (hALCs) using chemically defined culture conditions. Factors critical for the development of LCs were added to both culture systems. hLLCs expressed all steroidogenic genes and proteins important for T biosynthesis, synthesized T rather than cortisol, secreted steroid hormones in response to dibutyryl-cAMP and 22(*R*)-hydroxycholesterol, and displayed ultrastructural features resembling LCs. By contrast, hALCs synthesized cortisol rather than T. The success in generating hiPSC-derived hLLCs with broad human LC (hLC) features supports the potential for hiPSC-based hLC regeneration.

human Leydig cells | human induced pluripotent stem cells | differentiation | steroidogenesis | testosterone

Human pluripotent stem cells (hPSCs), including human embryonic stem cells (hESCs) and human induced pluripotent stem cells (hiPSCs), have the potential to differentiate into any somatic cell type (1). hESCs are the widely used hPSCs in developmental studies, whereas their application in regenerative medicine is impeded by ethical concerns and technical issues. Instead, hiPSCs, induced from somatic cells, have become a promising source for autologous cell therapies and disease modeling studies without the ethical concerns of hESCs.

Testicular Leydig cells (LCs) produce testosterone (T) in response to pituitary luteinizing hormone (LH) and its replacement human CG (hCG), both binding to the LH/choriogonadotropin (LHCGR) receptor (2). T formation involves the metabolism of a number of substrates, beginning with cholesterol, by enzymes in the mitochondria and smooth endoplasmic reticulum (2, 3). Reduced serum T, or hypogonadism, affects millions of men. The condition is common in aging men, with 20 to 50% of men over age 60 y reporting serum T levels significantly below those of young men (age 20 to 30 y) (4–6). Age-related declines in serum T levels are typically not a response to reduced LH, but rather a consequence of LCs becoming less responsive to LH, a condition referred to as primary hypogonadism that also occurs in many infertile men (6). Administering exogenous T, known as T-replacement therapy, reverses many of the symptoms of low T levels. However, flooding the body with high concentrations of stable T derivatives can pose a risk for aging males due to possible prostate (benign prostatic hyperplasia; prostate cancer) and cardiovascular consequences. T administered by gels and other transdermal methods have additional side effects of skin irritation and T transfer to sexual partners via skin contact. Moreover, the administration of exogenous T by any means can suppress LH and result in the suppression of spermatogenesis. Thus, the exogenous administration of T to ameliorate hypogonadism is inappropriate for men wishing to father children (6). For these reasons, there is a need for developing methods to obtain transplantable T-producing cells that could treat hypogonadism by reestablishing T-producing cell lineages in the body.

In humans, T is synthesized by LCs, deriving from mesenchymal cells of mesonephric origin (7–9). Although human mesenchymal stem cells (MSCs) have been successfully induced into human LCs (hLCs) (10–12), there are limitations in the numbers of MSCs that can be isolated and the associated potential trauma to donors, hindering the wide application of this approach to clinical therapies. Alternatively, hiPSCs, which are highly expandable in cell culture and have the potential to differentiate into all somatic cell

Significance

Our results suggest that both androgen- and cortisol-producing human Leydig and adrenal cells can be induced from human induced pluripotent stem cells. This bidirectional approach offers insights into the events specifying different steroidogenic cell populations sharing developmental origins. More importantly, our study provides a way to generate possible transplantation materials for clinical therapies. Human Leydig-like cells could also be useful for in vitro studies of testicular development and pathologies of testis-relevant diseases, and for the discovery of new drugs inducing androgen formation for hypogonadism treatment.

Author contributions: L.L., Y.L., M.C., and V.P. designed research; L.L., Y.L., J.F., Y.H., and G.C. performed research; C.S. and V.P. contributed new reagents/analytic tools; L.L., M.C., J.F., H.E.C., and V.P. analyzed data; and L.L., H.E.C., and V.P. wrote the paper.

The authors declare no competing interest.

This article is a PNAS Direct Submission.

See Commentary on page 22904.

[1]To whom correspondence may be addressed. Email: vpapadop@usc.edu.

This article contains supporting information online at www.pnas.org/lookup/suppl/doi:10.1073/pnas.1908207116/-/DCSupplemental.

First published October 7, 2019.

types, are an emerging source of autologous cell therapies (13). Previous attempts have successfully induced hiPSCs into human adrenal-like cells (hALCs) (14), while human Leydig-like cells (hLLCs) remain unobtainable. Therefore, there is an urgent need to generate hLLCs, especially for treating hypogonadal men.

Mouse LCs and hLCs were induced from mouse MSCs using Nuclear Receptor Subfamily 5 Group A Member 1 (NR5A1/SF-1), the master gene of steroidogenesis (15), and shown to be closely related based on their expression of most steroidogenic genes (10–12). hCG and cyclic adenosine monophosphate (cAMP), known to be essential for steroidogenesis, have also been used to induce steroidogenic cells because of their long-half life and stability compared to LH, respectively (11, 14). Moreover, recombinant protein desert hedgehog (DHH) has been reported as an important factor for both proliferation and differentiation of rat stem LCs (16) and shown to increase T production after Leydig stem cells have been s.c. autografted into mice (17).

Here, we developed a strategy to differentiate hiPSCs into hLLCs by first deriving early mesenchymal progenitors (EMPs) and then deriving hLLCs through overexpression of SF-1 and in the presence of dibutyryl-cAMP (dbcAMP), DHH, and hCG. These hLLCs expressed hLC-related steroidogenic genes and had an overall hLC-similar gene expression pattern. Beyond gene expression, these cells also produced all of the steroidogenic enzymes essential for T biosynthesis. Moreover, the distinct ultrastructure of hLLCs, including enriched mitochondria and smooth endoplasmic reticulum and moderate amounts of lipid droplets, is evidence in support of their steroidogenic identity. More importantly, hLLCs secreted T in a stimulus-dependent manner, suggesting their functional maturation. These results demonstrate the feasibility of studying hLCs in vitro and pave the way for transplantation as a therapy for male hypogonadism using autologous hLLCs.

Results

Generation of hLLCs and hALCs by Different Culture Methods. On the basis of known embryological sequence of events, we defined a 2-stage framework for the differentiation of hiPSCs into either hLLCs or hALCs, including the expression of genes that mark the 2 distinct fates (Fig. 1*A*). To assess whether this developmental process could be recapitulated in vitro, we first induced hiPSCs into EMPs, which are the progenitor population for both LCs and ACs (18). Two days before EMP induction, hiPSC colonies were adapted to single-cell culture on Matrigel-coated plates using mTeSR medium (Fig. 1*B*). From induction day (ID) 0 to 6, EMPs were induced using a chemically defined medium (*SI Appendix*, *Methods*) on Matrigel-coated plates (Fig. 1*B*). The appearance of EMPs was evidenced by low expression levels of pluripotency markers (OCT4 and NANOG) and primitive streak markers (MIXL1 and TBXT) and high expression levels of EMP marker PDGFRA (19, 20) (Fig. 1*C*). Interestingly, EMPs also expressed COUP-TFII, which has been proposed as a potential marker for steroidogenic cells (21, 22), suggesting that EMPs might already be primed to differentiate into steroidogenic cells. Both expression levels of MSC markers (CD 73, CD 105, and CD 90) and steroidogenic genes were not up-regulated in EMPs (*SI Appendix*, Fig. S1*A*), suggesting that they were more like MSC progenitors rather than mature MSCs or steroidogenic cells.

There are ample studies that have successfully induced either hLLCs or hALCs from MSCs (10–12, 23). We therefore questioned whether steroidogenic cells, especially hLLCs, could be induced from EMPs. To search for the most likely factor triggering hLLC differentiation, we performed an Ingenuity Pathway Analysis (IPA) via input of all reported LC development-related factors (*SI Appendix*, Fig. S1*B*). As a result, 4 factors that play critical regulatory roles in LC development were located in the center of the network, including SF-1, DHH, hCG, and cAMP. Remarkably, IPA pointed to DHH as an essential factor for LC development, since it can trigger the overexpression of SF-1 and the secretion of and T (17, 24) (*SI Appendix*, Fig. S1*B*).

At the second induction stage, we examined whether these 4 factors could direct EMPs to hLLCs in different culture systems (Fig. 1*B*). On ID 6, EMPs were passaged to MesenCult-ACF Attachment Substrate (ACF)-coated plates using MesenCult-ACF medium (Fig. 1 *B*, *Top*). On ID 12, EMPs were transfected with an SF-1 expression vector and cultured in MesenCult-ACF medium with the addition of DHH, hCG, and cAMP (hereafter called the ACF-SF1 system). The transfection efficiency was indicated by using green fluorescent protein (GFP) as a reporter gene (*SI Appendix*, Fig. S1 *C*, *Left*). On ID 26, induced cells expressed SF-1 and showed an obvious up-regulation of cytochrome P450 family (CYP) 11 subfamily A member 1 (CYP11A1), hydroxy-delta-5-steroid dehydrogenase, 3 beta- and steroid delta-isomerase 2 (HSD3B2), CYP17A1, CYP11B1, and CYP11B2 in comparison to hiPSCs (Fig. 1*D*). Although CYP21B, an adrenal-specific steroidogenic gene, was not increased significantly, perhaps due to its comparable levels in hiPSCs and differentiated cells (Fig. 1*D*), the expression of steroidogenic genes in cells induced by the ACF-SF1 system was similar to that of reported hALCs (14).

To identify whether hALCs or hLLCs were induced by the ACF-SF1 system, we measured steroid hormones secreted from these cells. In humans, cortisol (CORT) and aldosterone (ALDO) are synthesized mainly by ACs, while T is synthesized mainly by LCs. The results revealed that these cells produced large amounts of CORT and ALDO (Fig. 1*E*) compared to T ($P < 0.01$), suggesting that the cells were induced into hALCs by the ACF-SF1 system, in agreement with previous data demonstrating that hACs could produce large amounts of CORT and ALDO and small amounts of T (25, 26). In addition, immunofluorescent staining analysis showed that 64.15 ± 19.59% of differentiated cells induced by ACF-SF1 system expressed CYP21B (*SI Appendix*, Fig. S2 *A*, *Bottom*, and *SI Appendix*, Fig. S2*B*), suggesting that the majority of the cells had differentiated into hALCs.

Since the ACF-SF1 system induced EMPs into hALCs, we investigated whether hLLCs could be induced from EMPs by different treatments. In mammal LC development, the appearance of collagen type I (COLI) in the testis accompanies LC maturation and the onset of T production (27). Moreover, a COLI coating method in combination with F12/DMEM containing 10% FBS (F12/FBS medium) has been used to induce steroidogenic cells from mesodermal cells (14). Accordingly, we hypothesized that a COLI coating together with F12/FBS medium and 4 factors (SF-1, DHH, hCG, and cAMP) could induce hLLC development. To test this hypothesis, on ID 6, EMPs were passaged to COLI coated plates using F12/FBS medium (Fig. 1 *B*, *Bottom*). On ID 8, cells were transfected with SF-1 constructs (*SI Appendix*, Fig. S1 *C*, *Right*) and cultured with F12/FBS medium containing dbcAMP, DHH, and hCG (hereafter called the COLI-SF1 system). On ID 22, SF-1–overexpressing cells showed high expression levels of CYP11A1, HSD3B2, CYP17A1, HSD17B3, CYP11B1, CYP11B2, and CYP19A1 (Fig. 1*F*). Specifically, HSD17B3, which is important for T biosynthesis, and CYP19A1, which converts T into estrogen, were expressed at higher levels in these cells compared to hALCs (*SI Appendix*, Fig. S2*C*), suggesting that the steroidogenic gene expression patterns of cells induced by the COLI-SF1 system were more similar to hLCs than hACs.

To assess whether hLLCs were successfully induced by the COLI-SF1 system, we measured the steroids secreted by these cells. ELISA results showed that these cells produced great amounts of T and minimal amounts of CORT and ALDO (Fig. 1*G*). In comparison to hALCs, these cells produced much higher levels of T ($P < 0.01$; *SI Appendix*, Fig. S2*D*), but significantly less CORT ($P < 0.0001$; *SI Appendix*, Fig. S2*E*), indicating that hLLCs and hALCs were differentially induced by the COLI- and ACF-SF1 systems, respectively. These data suggest that these

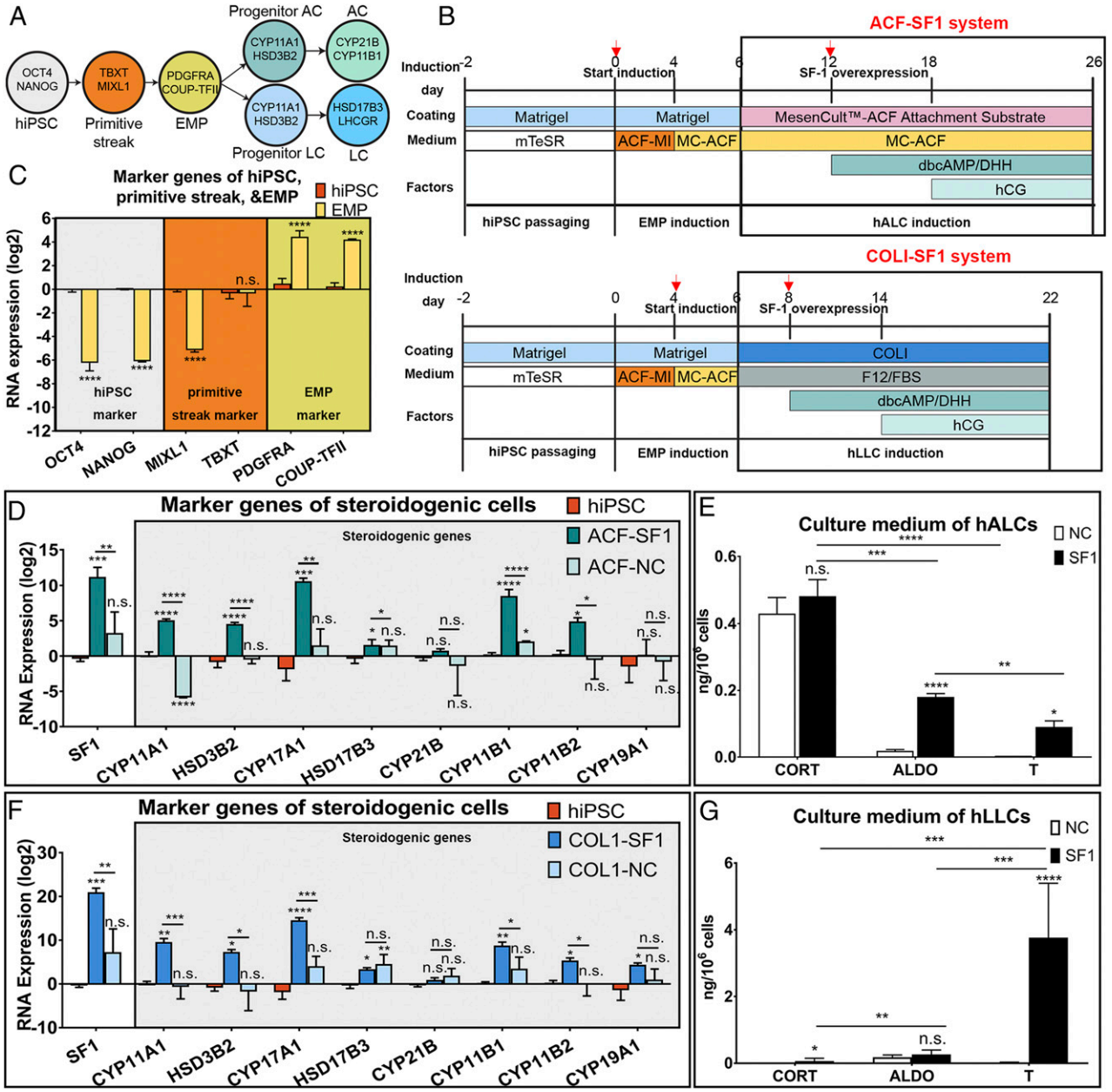

Fig. 1. Induction of human Leydig-like cells (hLLCs) and human adrenal-like cells (hALCs) from human induced pluripotent stem cells (hiPSCs). (*A*) Schematic of differentiation stages from hiPSCs into human adrenal cells (hACs) or human Leydig cells (hLCs). Genes displayed in each stage represent cellular markers of that stage. EMP, early mesenchymal progenitors. (*B*) Schematic strategy for the induction hALCs and hLLCs from hiPSCs. Before the specification of hALCs and hLLCs, hiPSCs were first induced into EMPs. At 2 d before the EMP induction, hiPSCs were plated on Matrigel-coated plates and cultured in mTeSR medium for proliferation. On induction day (ID) 0, cells were cultured in STEMdiff-ACF Mesenchymal Induction (ACF-MI) medium for 4 d and MesenCult-ACF (MC-ACF) medium for 2 d to form EMPs. (*Top*) hALCs were induced from EMPs by the ACF-SF1 system. On ID 6, EMPs were transferred to MesenCult-ACF Attachment Substrate-coated plates and cultured in MC-ACF medium. On ID 12, EMPs were transfected with SF-1 plasmid and exposed to dibutyryl-cAMP (dbcAMP) and desert hedgehog (DHH) in MC-ACF medium for 6 d. On ID 18, cells were exposed to dbcAMP, DHH, and human CG (hCG) in MC-ACF medium for 8 d. On ID 26, hALCs formed. (*Bottom*) hLLCs were induced from EMPs by the COLI-SF1 system. On ID 6, EMPs were transferred to Collagen type I (COLI)-coated plates and cultured in F12/DMEM supplemented with 10% FBS (F12/FBS) for 2 d. On ID 8, cells were transfected with SF-1 plasmid and exposed to dbcAMP and DHH in F12/FBS medium for 6 d. On ID 14, cells were exposed to dbcAMP, DHH, and hCG in F12/FBS medium for 8 d. On ID 22, hLLCs formed. (*C*) qRT-PCR analyses of hiPSC markers (OCT4 and NANOG), primitive streak markers (MIXL1 and TBXT), and EMP markers (PDGFRA and COUP-TFII) from hiPSCs and EMPs. The low expression of OCT4, NANOG, MIXL1, and TBXT indicate that EMPs have lost pluripotency and passed the primitive streak stage. The high expression of PDGFRA and COUP-TFII indicates the appearance of EMPs. (*D* and *F*) qRT-PCR analyses of steroidogenic cell markers in hiPSCs, hALCs, and hLLCs, respectively. Both hALCs and hLLCs highly expressed SF-1. hALCs highly expressed many steroidogenic genes but not the adrenal-specific gene CYP21B and testis-specific genes HSD17B3 and CYP19A1, in comparison to hiPSCs. The insignificant up-regulation of CYP21B in hALCs might be due to its detectable expression level in both hiPSCs and hALCs that is shown in *SI Appendix*, Fig. S2*A*, suggesting gene expression in hALCs is similar to that of hACs. hLLCs highly expressed most of the steroidogenic genes except for CYP21B, suggesting their gene expression is similar to that of hLCs. (*E* and *G*) ELISAs measuring cortisol (CORT), aldosterone (ALDO), and testosterone (T) in cell supernatants of hALCs and hLLCs, respectively. hALCs produced significantly more CORT and ALDO than T, while hLLCs produced significantly more T than CORT and ALDO. NC, GFP-transfected negative control cells. The quantitative comparison of T and CORT produced by hALCs and hLLCs is shown in *SI Appendix*, Fig. S2 *D* and *E*. Data in *C*–*G* are presented as mean ± SD, $n = 3$. In *D* and *F*, *P* value was generated by ANOVA. Multiple comparisons were corrected by Tukey's *t* test. In *E* and *G*, *P* value was generated by the Student's *t* test. n.s., not significant at $P > 0.05$ (*$P < 0.05$, **$P < 0.01$, ***$P < 0.001$, and ****$P < 0.0001$).

2 protocols can drive EMPs from hiPSCs to a distinct cell fate, namely hALCs or hLLCs.

hLLCs and hALCs Display Differential Gene Expression Patterns. To further characterize hLLCs and hALCs, we performed a microarray analysis comparing transcriptome expression profiles of hLLCs and hALCs cells with that of hiPSCs. In total, 21,448 transcripts were detected in the arrays. A principal components analysis showed that the variability across the 3 cell populations was large (*SI Appendix*, Fig. S3*A*). A 2-way hierarchical clustering analysis further confirmed that each cell population displayed a distinct gene expression pattern (*SI Appendix*, Fig. S3*B*).

To reveal differentially expressed (DE) transcripts with statistical significance in each population, we used a cutoff of absolute fold-change (FD) > 2 and false discovery rate (FDR) < 0.05 to filter all transcripts. The filtration identified a total of 5,087 DE transcripts in aggregate from the 3 cell types (Dataset S1). We then performed a hierarchical clustering analysis of DE transcripts and found 3 clusters that were specifically expressed in each cell type (Fig. 2*A* and Dataset S2). These clusters included 437 transcripts in hLLCs (Fig. 2*A*, yellow box), 311 transcripts in hALCs (Fig. 2*A*, purple box), and 2,550 transcripts in hiPSCs (Fig. 2*A*, green box). To validate the array data, we selected 3 genes that are important for hLLCs and hALCs on which to perform qRT-PCR analyses. The transcripts of steroidogenic acute regulatory protein (STAR) and LHCGR, which are essential markers of mature hLCs, were highly expressed in hLLCs (*SI Appendix*, Fig. S4 *A* and *B*). However, the transcript of melanocortin 2 receptor (MC2R), the essential marker of hACs, was only insignificantly up-regulated in hALCs (*SI Appendix*, Fig. S4*C*), suggesting the functional immaturity of these cells, despite the production of CORT and ALDO.

Next, we performed an IPA to determine the biological functions associated with each cluster. The genes highly expressed in hLLCs were substantially involved in steroidogenesis-associated processes, such as the synthesis and/or metabolism of lipid, pregnenolone (P5), progesterone (P4), androstenedione (A4), and dihydrotestosterone (DHT; *SI Appendix*, Fig. S4*D* and Dataset S3). This specific transcript expression pattern suggested active steroidogenesis in hLLCs. On the contrary, hALC-specific expressed genes were only related to cellular movement, cell-to-cell signaling, and cellular development (*SI Appendix*, Fig. S4*E*, and Dataset S3), again suggesting their functional immaturity. Particularly, the genes involved in cellular development were strongly related to the differentiation of connective tissue cells and vascular cells, suggesting the developmental potential of hALCs toward the adrenal gland (Dataset S3). Distinct from both steroidogenic cell types, hiPSCs showed a unique gene expression pattern that was highly related to stemness, including cell cycle and DNA replication processes (*SI Appendix*, Fig. S4*F*).

Steroidogenic Pathways Are Differentially Activated in hLLCs and hALCs. To further confirm the identity of the hiPSC-derived cells as steroidogenic cells, we performed a detailed comparison across the 3 cell types of functional pathways related to steroidogenesis, including the protein kinase A (PKA) signaling pathway, cAMP-mediated signaling pathway, lipid droplet-associated functions, cholesterol biosynthesis, pregnenolone biosynthesis, androgen signaling pathway, androgen biosynthesis, and glucocorticoid biosynthesis. Analyses revealed that many of the genes involved in the cAMP/PKA pathway were expressed more highly in hLLCs and hALCs in comparison to hiPSCs (Fig. 2*B* and Dataset S4), including G protein-coupled receptors, adenylyl cyclase, cyclic nucleotide phosphodiesterase, PKA, cAMP-response element-binding protein, and cAMP-responsive modulator, suggesting that the cAMP/PKA pathway has been substantially activated for steroidogenesis in these cells. Furthermore, most of the genes involved in signaling pathways/biosynthesis of steroids (pregnenolone and other androgens) were expressed the highest in hLLCs in comparison to the other 2 cell types (Fig. 2*B* and Dataset S4). Besides genes involved in both androgen and glucocorticoid biosynthesis (from pregnenolone to 17α-hydroxyprogesterone), only genes involved in glucocorticoid biosynthesis were not up-regulated in hALCs (Fig. 2*B* and Dataset S4), indicating their low capacity for glucocorticoid production. Many DE genes related to lipid droplets were highly expressed in both hLLCs and hALCs, while those involved in cholesterol biosynthesis were down-regulated (*SI Appendix*, Fig. S4*G* and Dataset S4). qRT-PCR results confirmed expression trends of the most up-regulated genes in hLLCs and hALCs with regard to each pathway (*SI Appendix*, Fig. S5 *A*–*I*), further confirming the array data.

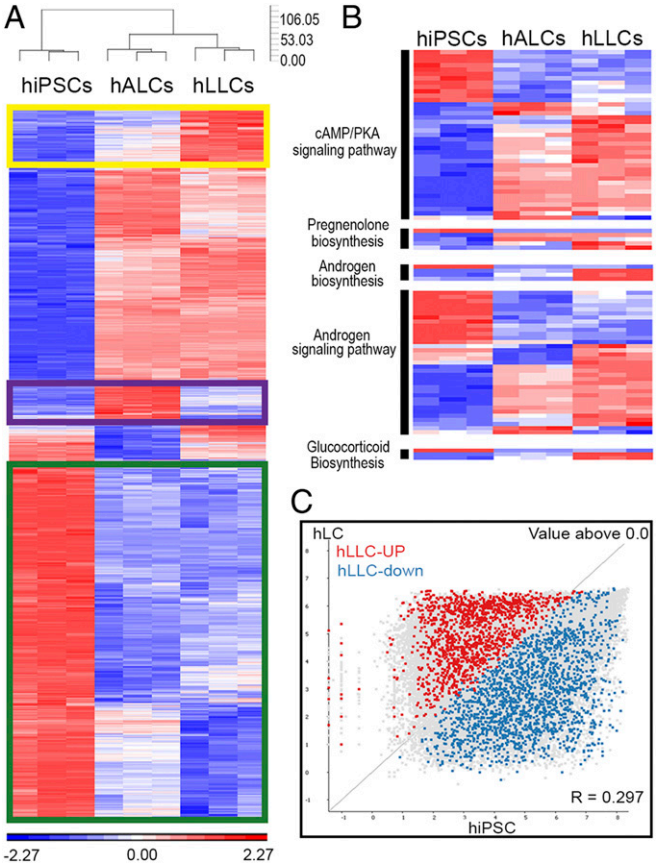

Fig. 2. Microarray analyses comparing hLLCs with hALCs and hiPSCs. (*A*) The dendrogram showing the hierarchical clustering of transcriptome expression profiles as measured by microarray analyses for biological replicates of hiPSCs, hALCs, and hLLCs. The transcriptome expression of hLLCs is more similar to that of hALCs compared to hiPSCs. Distances between samples were measured using the average linkage and Euclidean distance metric. Heat map summarizing the expression of 5,087 transcripts that show differential expression (absolute fold change [AFC] > 2 and false discovery rate [FDR] < 0.05) across the sample groups. The yellow, purple, and green boxes indicate clusters of transcripts that were specifically expressed in hLLCs, hALCs, and hiPSCs, respectively. (*B*) Heat map displaying the expression of selected differentially expressed transcripts in each of the indicated categories. Note that most of genes involved in indicated pathways/biosynthesis were expressed the highest in hLLCs, supporting their steroidogenic functions. (*C*) Comparison of the expression of transcripts in hLLCs, hLCs, and hiPSCs. The gray dots falling into the upper left triangle of the scatter plot represent transcripts more highly expressed in hLCs versus hiPSCs, while the gray dots falling into the bottom right triangle represent transcripts more highly expressed in hiPSCs versus hLCs. A total of 300 differentially expressed (DE) transcripts (AFC > 5 and FDR < 0.05) identified in the comparison of hLLCs versus hiPSCs fall into the upper left triangle (red dots) and are therefore are more similar to hLC expression than hiPSCs. In the contrast, 310 DE transcripts fall into the bottom right triangle (blue dots) and are therefore are more similar to hiPSC expression than hLCs.

The low expression of cholesterol biosynthesis-related genes and high expression of lipid droplet-associated genes in hLLCs and hALCs (*SI Appendix*, Fig. S4*G*) suggested that they might take up cholesterol from extracellular lipoproteins and store them in intracellular lipid droplets (28). Via the cAMP-dependent signaling pathway, cholesterol is transferred through the transduceosome to the outer mitochondrial membrane (29). Our array data showed that PKAR1A and ABCD3, which are components of transduceosome, were up-regulated in both hLLCs and hALCs (Dataset S5), while STAR, another important component, was specifically expressed in hLLCs (Dataset S5). In contrast, the level of the cholesterol-binding mitochondrial TSPO remained unchanged. Additionally, RAB18, the lipid droplet-surface protein, and ACSL1, which regulates the import of lipid into mitochondria (29), were increased in both hLLCs and hALCs (Dataset S5), while ATAT1, present in the endoplasmic reticulum and associated with lipid droplets, was only increased in hLLCs (Dataset S5). Besides lipid droplets, the endoplasmic reticulum can also deliver cholesterol to mitochondria via mitochondria-associated membranes. According to array results, genes encoding mitochondria-associated membrane-located proteins, including IP3R/ITPR1, MFN2, and ATAD3C, were up-regulated in both hLLCs and hALCs (Dataset S5), while other genes, such as ACSL4, ATAD3A, and PACS2, were specifically up-regulated in hLLCs (Dataset S5). In particular, the up-regulation of MFN2, which is also a mitochondrial shaping protein, suggested activation of steroidogenesis in mitochondria (29). The finding that many genes involved in cholesterol transport were only up-regulated in hLLCs suggests that such a function might be more active in hLLCs.

hLLCs and hLCs Show Highly Similar Transcriptome Expression Patterns. Because our focus was to induce hiPSCs into hLLCs rather than hALCs, we continued with the characterization of hLLCs. To reveal the similarities between hLLCs and hLCs, we compared their transcriptome expression patterns. Based on the published transcriptome data from hiPSCs (Gene Expression Omnibus accession ID GSE117664) and hLCs (GSE74896) (30), we found that one cluster of transcripts was specifically expressed in hiPSCs (Fig. 3*C*, gray dots in the bottom right triangle, and *SI Appendix*, Fig. S6*A*, C1), while another cluster of transcripts was specifically expressed in hLCs (Fig. 3*C*, gray dots in the top left triangle, and *SI Appendix*, Fig. S6*A*, C3).

We then compared the specifically expressed transcripts identified from published transcriptome data to the transcripts that were drastically changed in hLLC differentiation (absolute FD > 5 and FDR < 0.05). The comparison showed that 300 C3 transcripts (Fig. 2*C*, red dots in the top left triangle, and Dataset S6) and 310 C1 transcripts (Fig. 2*C*, blue dots in the bottom right triangle, and Dataset S6) were differentially expressed during the induction of hLLCs. Analyzing the drastically changed transcripts, we identified 151 transcripts (36.7% of up-regulated transcripts in hLLCs and 55.5% of up-regulated transcripts in hLCs) consistently up-regulated in both hLLCs and hLCs (*SI Appendix*, Fig. S6 *B*, *Left*, and Dataset S7) and 177 transcripts (48.5% of down-regulated transcripts in hLCs and 79.7% of down-regulated transcripts in hLLCs) consistently down-regulated in both hLLCs and hLCs (*SI Appendix*, Fig. S6 *B*, *Right*, and Dataset S7). These results suggested that the whole transcriptome expression pattern of hLLCs was very similar to that of hLCs.

hLLCs Display Steroidogenic Enzyme Patterns. Beyond the gene expression pattern, we measured the protein expression pattern of hLLCs. Immunohistochemistry staining results showed that 93.08 ± 4.21% of cells expressed HSD3B2 (Fig. 3 *A* and *B*), which is the cellular marker of both fetal and adult hLCs, and 57.02 ± 9.47% of cells expressed HSD17B3, which is the cellular marker only for adult LCs (Fig. 3*A*) (31, 32), suggesting that the vast majority of cells differentiated toward hLCs and approximately half of them became adult hLCs. Moreover, some differentiated cells expressed both HSD3B2 and LHCGR (Fig. 3*B*), indicating that the function of a portion of hLLCs is regulated by hCG/LH.

Western blot analyses of hLLCs or hiPSCs showed up-regulated expression of SF-1 in hLLCs (Fig. 3*C* and *SI Appendix*, Fig. S7 *A* and *B*). Furthermore, de novo expression of CYP11A1 and up-regulation of HSD3B2 and CYP17A1 were detected in hLLCs (Fig. 3*C* and *SI Appendix*, Fig. S7*C*). The expression of LHCGR was detected in hiPSCs and hLLCs (Fig. 3*C* and *SI Appendix*, Fig. S7*C*). Both 37-kDa- and 25-kDa-size STAR were detected by Western blot (Fig. 3*C* and *SI Appendix*, Fig. S7*D*). However, the 25-kDa-size STAR was specifically expressed in hLLCs and a human adrenal cell line (H295) but not hiPSCs. To confirm that the 25-kDa-size STAR was the mature form of STAR that could be formed upon cAMP treatment (33), we treated H295 cells with dbcAMP for 3 h and observed an increase of 25-kDa-size STAR that confirmed its identity (Fig. 3*C* and *SI Appendix*, Fig. S7*E*). Therefore, the expression of LHCGR and the mature form of STAR in hLLCs suggested that hLLCs should be able to transfer cholesterol into mitochondria in response to hCG/LH signaling as in normal steroidogenic cells.

HSD17B3 was only expressed in hLLCs but not hiPSCs or hALCs (Fig. 3*D* and *SI Appendix*, Fig. S8*A*), confirming that only hLLCs were similar to adult LCs. In contrast, CYP21B was expressed highly in hiPSCs and hALCs but less in hLLCs (Fig. 3*D* and *SI Appendix*, Fig. S8*B*), confirming that hLLCs favored the steroidogenic pathway leading to T biosynthesis rather than CORT biosynthesis. Furthermore, OCT4 was undetectable in both hLLCs and hALCs (Fig. 3*D* and *SI Appendix*, Fig. S8 *C* and *D*), confirming the loss of stemness in these steroidogenic cells.

hLLCs Show hLC-Like Ultrastructure. We next compared the ultrastructure of hLLCs with the original hiPSCs. As shown in Fig. 3 *E* and *F* and *SI Appendix*, Figs. S9 and S10, hLLCs showed condensed smooth endoplasmic reticulum that was contiguous with the nuclear membrane and extended throughout the cell, a hallmark of hLCs. In contrast, hiPSCs contained more free ribosomes with scarce portions of smooth endoplasmic reticulum (*SI Appendix*, Fig. S13 *A–F*) (34). Another specific structure in hLLCs was the swirled variety of smooth endoplasmic reticulum that is myelin sheath-like and predominantly present in LCs of many species (Fig. 3*G* and *SI Appendix*, Fig. S11) (35). Other than smooth endoplasmic reticulum, plentiful elongated mitochondria were the most conspicuous morphological feature of hLLCs (Fig. 3 *E*, *G*, and *H* and *SI Appendix*, Figs. S9, S11, and S12). Mitochondrial cristae in hLLCs were well-defined with lamellar shapes. The lamellar cristae type is a feature of hLCs that has been reported before (36–38). Moreover, these mitochondria were very close together, to the exclusion of other organelles (Fig. 3 *G* and *H*), suggesting that these cells were differentiating toward typical steroidogenic cells. hiPSCs also possessed numerous mitochondria (*SI Appendix*, Fig. S13 *A–F*). However, in comparison to hLLCs, most of mitochondria in hiPSCs appeared spherical in shape with poorly developed cristae, suggesting an immature status (39). A distinct character of hiPSCs was the large ratio of nucleus to cytoplasm with 1 to 4 nucleoli per cell (34) (*SI Appendix*, Fig. S13 *A* and *D*). In addition, large nucleoli were observed more frequently in hiPSCs. Besides these morphological differences, both hLLCs and hiPSC contained lipid droplets (Fig. 3 *G* and *H* and *SI Appendix*, Fig. S13*E*) (34), though varied in phenotype and numbers. Rough endoplasmic reticulum and Golgi were also present in both cell types (Fig. 3 *E* and *F* and *SI Appendix*, Fig. S13 *C* and *F*). However, rough endoplasmic reticulum, which may relate to protein synthesis activity in hLCs, was more enriched in hLLCs compared to hiPSCs.

hLLCs Possess Steroidogenic Pathways of Testosterone Biosynthesis. As shown here earlier, hLLCs secreted T rather than CORT. We therefore assessed their metabolic intermediates from steroidogenic pathways leading to the synthesis of either T or CORT (Fig. 4*A*).

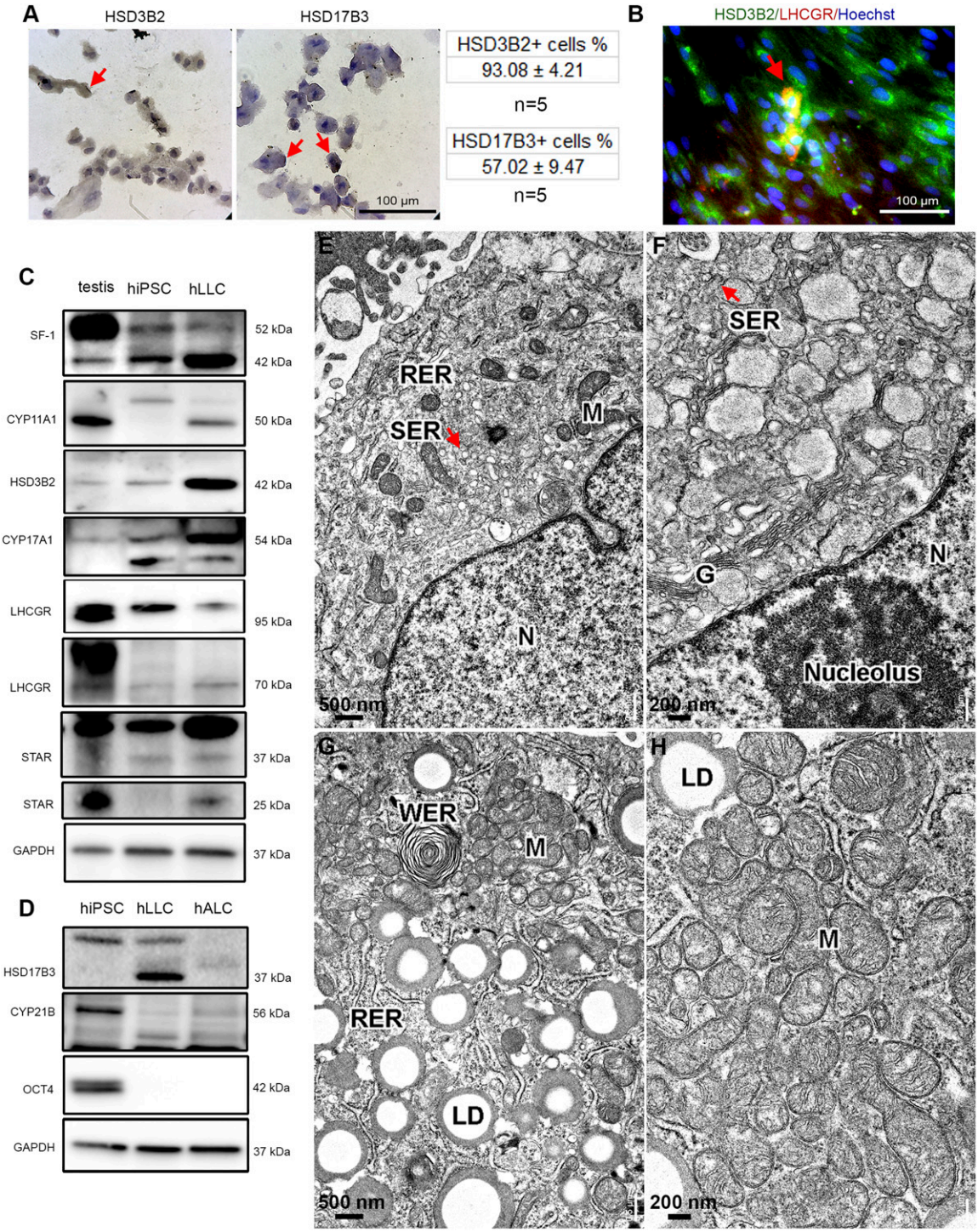

Fig. 3. Protein expression profile and ultrastructure of hLLCs. (*A*) Immunocytochemistry analyses of hLC marker HSD3B2 and adult LC marker HSD17B3. Cells with positive stains were indicated by arrows. The table next to them showed that the percentages of HSD3B2- and HSD17B3-positive cells were 93.08 ± 4.21% and 57.02 ± 9.47%, respectively. (Scale bar, 100 μm.) (*B*) Immunofluorescent staining of HSD3B2 (green channel) indicated that the vast majority of cells differentiated toward hLLCs. Some hLLCs also expressed LHCGR (red channel, indicated by arrow), suggesting that the function of some hLLCs is regulated by hCG/LH. (Scale bar, 100 μm.) (*C*) Western blot analyses of SF-1, CYP11A1, HSD3B2, CYP17A1, LHCGR, STAR, and GAPDH in hiPSCs and hLLCs. The results indicate that, upon the overexpression of SF-1, hLLCs highly expressed CYP11A1, HSD3B2, and CYP17A1, all of which are important for T biosynthesis. The presence of LHCGR and STAR implies that hLLCs could transfer cholesterol to mitochondria under the regulation of hCG/LH signaling. Human testicular lysate was used as a positive control. (*D*) Western blot analyses of HSD17B3, CYP21B, and OCT4 in hiPSCs, hLLCs, and hALCs. The specific expression of HSD17B3 in hLLCs indicates the hLC properties of hLLCs. The negligible expression of CYP21B in hLLCs suggests their poor synthetic capacity for CORT and ALDO. The undetectable expression of OCT4 in hLLCs and hALCs suggests that hiPSCs stemness had been eliminated. (*E–H*) Transmission electron microscopy images of hLLCs showing their ultrastructure. (*E–F*) hLLCs possessed condensed smooth endoplasmic reticulum (SER; indicated by arrow). (*G*) The swirled variety of SER (WER) is also found in hLLCs. (*G* and *H*) The presence of plentiful mitochondria (M) that were close together. Note that their cristae were more lamellar-like. Moderate amounts of lipid droplets (LDs), rough endoplasmic reticulum (RER), and Golgi (*G*) were also found in hLLCs. N, nucleus. (Scale bars: *E* and *G*, 500 nm; *F* and *H*, 200 nm.) The full-size TEM images are provided in *SI Appendix*, Figs. S9–S12.

We first evaluated the amount of P5, P4, dehydroepiandrosterone (DHEA), and A4 secreted into culture media. We found that hLLCs and hALCs secreted similar amounts of P5 (Fig. 4*B*). However, hALCs secreted more P4 (Fig. 4*C*), whereas hLLCs secreted more DHEA and A4 (Fig. 4 *D* and *E*). The variability of steroid products implies that hALCs might take the Δ4 steroidogenic pathway (P4 and A4) to synthesize ALDO and CORT, while hLLCs had no preference for synthesis of T.

Since hCG/LH regulated T production is critical for in vivo functions of hLLCs and hCG is used for the treatment of male hypogonadism (40, 41), we checked whether T production could be stimulated by hCG. Briefly, from ID 10 to 22, we compared the cell supernatants of the differentiated cells cultured with hCG/cAMP/DHH to those only cultured with DHH (Fig. 5*A*). At 48 h after the first treatment of hCG/cAMP (ID 16), T biosynthesis was significantly elevated ($P < 0.05$; Fig. 5*A*). The enhanced T response to hCG stimulation was sustained from ID 16 to 20. With continued culture of hCG/cAMP from ID 20 to 22, the cells remained responsive to hCG stimulation ($P < 0.01$), but the T concentrations declined and were not statistically different from that of ID 14. This overall change was highly consistent with in vivo data showing the effects of hCG treatment on rat LCs (42). To further clarify that hCG could acutely stimulate T production in hLLCs, we cultured differentiated cells with cAMP/DHH from ID 10 to 18 and then treated them with hCG for 1 h. A significant increase of T production was stimulated (Fig. 5*B*), supporting that T production in hLLCs could be regulated by hCG. In addition to that, we also detected increased levels of immunoreactive phospho-STAR in cells treated with hCG (*SI Appendix*, Fig. S14), although increased STAR phosphorylation is not necessarily linked to the steroidogenic activity of the protein (43, 44).

In hLCs, the binding of hCG/LH to LHCGR will stimulate the elevation of cAMP levels and the activation of PKA (45). The cAMP/PKA signaling cascade then activates the transduceosome and metabolon, which regulate the transfer of cholesterol from outer to inner mitochondrial membrane (29), where CYP11A1 converts cholesterol into P5 (Fig. 4*A*) (46). Since we observed the activation of the steroidogenic pathway in hLLCs, we checked whether they could be stimulated in response to cAMP signals. After hLLCs were treated with dbcAMP, the steroids secreted into the media were measured. Not surprisingly, T secretion was stimulated by dbcAMP significantly (Fig. 5*C* and *SI Appendix*, Fig. S15 *A–C*). Although the production of P5 and DHEA were significantly stimulated, no significant difference between stimulated Δ5 steroid (P5 and DHEA) and Δ4 steroids (P4 and A4) was observed (Fig. 5 *D–I*), suggesting that dbcAMP could stimulate hLLCs to synthesize T without favoring a specific steroidogenic pathway. A similar steroid production pattern has been observed when hLLCs were treated with 22(*R*)-hydroxycholesterol (*SI Appendix*, Fig. S16 *A–G*), further confirming the catalytic ability of steroidogenic enzymes in hLLCs.

To confirm that our induction strategy is applicable to multiple hiPSC lines with variable genetic background, we repeated the hLLC induction in a second hiPSC line (UCSD128i-7–5; WiCell). Both expression patterns of steroidogenic cell markers and T response to hCG stimulation of the second hiPSC-derived hLLCs were similar to that of the first one (*SI Appendix*, Fig. S17 *A–E*), supporting the reproducibility of our hLLC induction strategy.

Discussion

Despite advances in generating rodent LCs from iPSCs, human iPSC-derived LCs are still lacking. Here, we demonstrate that hiPSCs can be differentiated into EMPs and further directed to hLLCs using an induction strategy that is extremely concise and highly practical. Indeed, the overexpression of SF-1 in conjunction with only 3 factors and a COL1 coating method were sufficient to derive hLLCs from hiPSCs.

We report that the transient expression of SF-1, combined with hedgehog, PKA, and hCG, in both COLI- and ACF-SF1 systems could differentially induce EMPs into either hLLCs or hALCs, respectively. The predilection of the ACF-SF1 system to favor hALCs development may be a consequence of specific components of the ACF-SF1 system itself. It is possible that MesenCult-ACF medium (proprietary) contains much more CORT compared to the F12/FBS medium, and thus favors AC formation (47) while inhibiting the LC development (48). Other than CORT, unknown extracellular matrix components contained in the MesenCult-ACF Attachment Substrate, as well as their composition ratio, might also contribute to the differentiation of EMPs toward hALCs (49). A notable feature of the present protocol is the addition of DHH in the induction medium, which has rarely been used in the induction of human steroidogenic cells before. DHH is secreted by Sertoli cells and may have a critical role in stimulating both fetal LC and adult LC development (24, 50), as well as regulating steroidogenesis of LCs (51). More importantly, it has been shown to play a critical role in T recovery when Leydig stem cells were s.c. autografted into mice (17). We speculated that DHH together

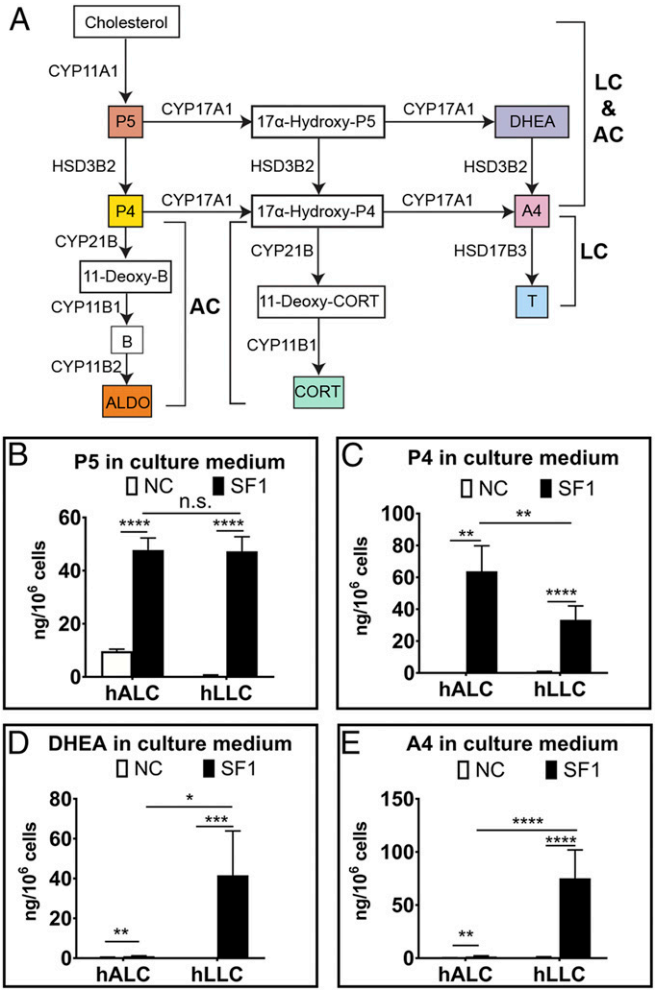

Fig. 4. Steroid production in hLLCs and hALCs. (*A*) Steroidogenic pathway in hALCs and hLLCs leading to the production of ALDO, CORT, and T. P5, pregnenolone; 17α-hydroxy-P5, 17α-hydroxy-pregnenolone; DHEA, dehydroepiandrosterone; P4, progesterone; 17α-Hydroxy-P4, 17α-hydroxy-progesterone; A4, androstenedione; 11-Deoxy-B, 11-deoxycorticosterone; B, corticosterone; 11-deoxy-CORT, 11-deoxycortisol. (*B–E*) ELISA analyses of P5, P4, DHEA, and A4 in the media of SF-1–overexpressing hALCs and hLLCs. Compared with hALCs, hLLCs produce similar amounts of P5 (*B*) and less P4 (*C*), but greater amounts of DHEA and A4 (*D* and *E*). NC, negative controls. Data are presented as mean ± SD, $n \geq 3$. *P* value was generated by the Student's *t* test. n.s., not significant at $P > 0.05$ (*$P < 0.05$, **$P < 0.01$, ***$P < 0.001$, and ****$P < 0.0001$).

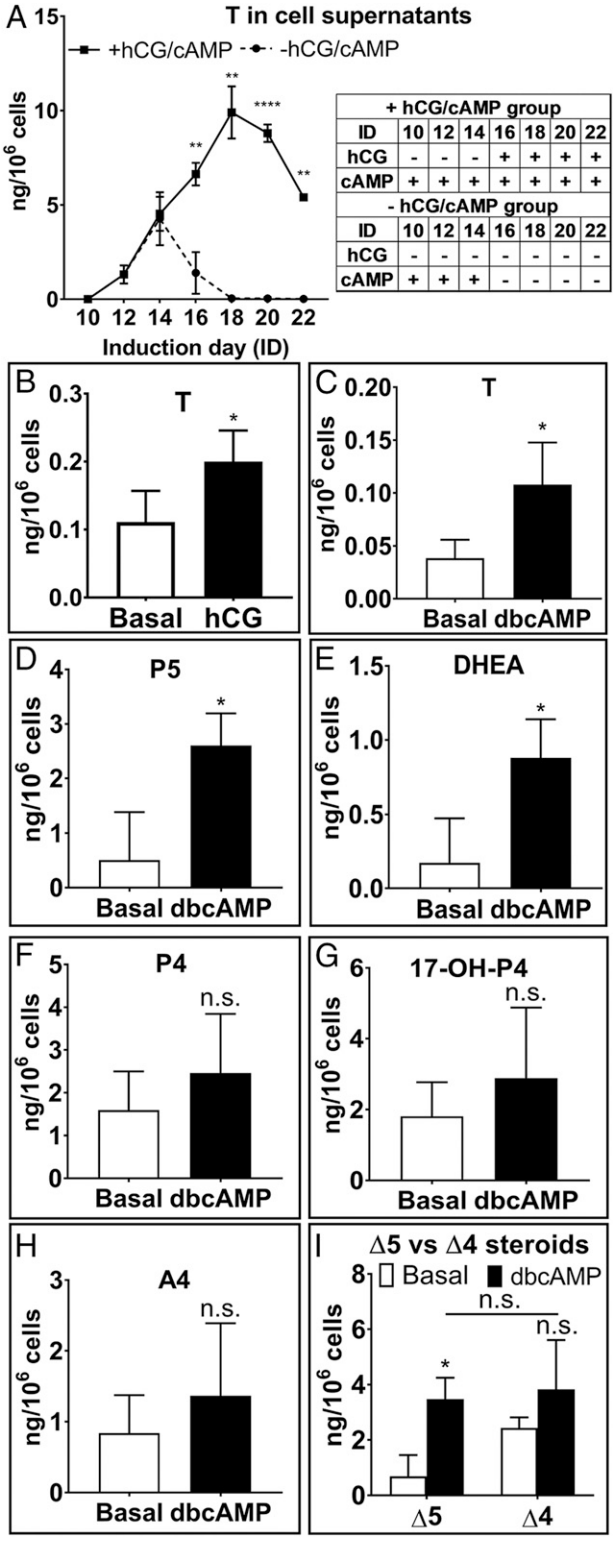

Fig. 5. Steroid production in hLLCs upon the stimulation of hCG and dibutyryl-cAMP. (*A*) ELISA analyses of T in the cell supernatants from ID 10 to 22. From ID 14 to 22, differentiated cells were cultured with F12/FBS medium containing either hCG/dbcAMP/DHH (+hCG/cAMP group) or DHH (-hCG/cAMP group). For comparison between groups, T concentrations were compared at ID 14, 16, 18, 20, and 22, and *P* values were generated by the Student's *t* test. n.s., not significant at $P > 0.05$ (*$P < 0.05$, **$P < 0.01$, ***$P < 0.001$, and ****$P < 0.0001$). For comparison within groups, T concentrations were compared across ID 14, 16, 18, 20, and 22, and *P* values were generated by ANOVA. Multiple comparisons were corrected by Tukey's *t* test. For +hCG/cAMP group, *P* value of ANOVA < 0.0001, T concentrations of ID 18 and 20 were significantly different from that of ID 14 ($P < 0.05$). For –hCG/cAMP group, *P* value of ANOVA < 0.0001; T concentrations at ID 16, 18, 20, and 22 were significantly different from that at ID 14 ($P < 0.001$). (*B*) ELISA analyses of T in the cell supernatants on ID 18. Cells were cultured with only DHH and dbcAMP from ID 8 to 18. Thereafter, cells treated with 150 ng/mL hCG for 1 h secreted significantly more T than cells without hCG treatment. (*C*) ELISA analyses of T in the cell supernatants. hLLCs treated with 1 mM dbcAMP for 3 h secreted significantly more T than hLLCs without dbcAMP. (*D–H*) LC-MS/MS analyses of steroids in the cell supernatants. hLLCs treated with dbcAMP secreted significantly more P5 and DHEA than hLLCs without dbcAMP. (*I*) Sum of the Δ5 steroids (P5 and DHEA) and Δ4 steroids (P4 and A4) in cell supernatants of hLLCs with or without dbcAMP. There is no significant difference between the amounts of Δ5 and Δ4 steroids that were stimulated by dbcAMP. Data in *B–I* are presented as mean ± SD, $n \geq 3$. *P* value was generated by the Student's *t* test. n.s., not significant at $P > 0.05$ (*$P < 0.05$, **$P < 0.01$, ***$P < 0.001$, and ****$P < 0.0001$).

with SF-1 expression could stimulate hLC development in vitro. Although our results strongly support this hypothesis, it should be confirmed in the future by testing the time-dependent effects of DHH during hLLC differentiation and using a gain- and loss-of function study to determine whether DHH is associated with hLC development (16, 17, 50).

HSD17B3 is the enzyme that specifically metabolizes A4 to T in the steroidogenic pathway, whereas CYP21B is involved in CORT and ALDO synthesis. Protein expression analyses revealed a very high expression of HSD17B3 protein, while CYP21B protein was barely detectable. This protein profile is consistent with the differential secretion levels of T and CORT. Beyond its critical role in T biosynthesis, HSD17B3 is also the specific marker of adult LCs (31, 32). Immunohistochemistry staining results showed that 93.08 ± 4.21% of differentiated cells expressed HSD3B2 while only 57.02 ± 9.47% of differentiated cells expressed HSD17B3, indicating that approximately half of cells were likely adult LCs and the rest of cells were likely immature LCs.

In hLLCs, we found some proteins present in variable forms. For example, due to massive glycosylation, there are 2 sizes of LHCGR proteins (52). However, the mature, cell-membrane form of LHCGR (95 kDa) was expressed less in hLLCs compared to hiPSCs. In addition to LHCGR, we also detected 2 different band sizes of SF-1. Although the 42-kDa-size SF-1 has been less reported, it has been seen in SF-1–overexpressing cells (12, 53). In addition, we found both the premature (37 kDa) and mature forms (25 kDa) of the STAR protein in steroidogenic cells (hLLCs, testicular cells, and H295 cells) (54), whereas hiPSCs contained only the premature forms. This result suggests that, in steroidogenic cells, STAR is cleaved and imported into mitochondria as cells acquire steroidogenic competency during development (54), and also that steroidogenic mitochondria have the necessary proteases to cleave STAR to its mature form.

To fully characterize hLLCs, we compared their ultrastructure with hiPSCs. Beyond distinct characteristics, such as the large amount of smooth endoplasmic reticulum and the presence of myelin sheath-like structures in hLLCs, and numerous ribosomes, a high nucleo-cytoplasmic ratio, and the presence of chromatin in hiPSCs, both contained plenty of mitochondria. The appearance of mitochondria in hiPSCs was in accordance with increased aerobic glycolysis and metabolism (55). Moreover, both cell types presented lipid droplets, Golgi, and rough endoplasmic reticulum. These organelles are generally found in hLCs (56), in which lipid droplets are known to provide cholesterol for steroidogenesis and Golgi participate in glycoprotein secretion (57, 58). However, their functions in hiPSCs remain unclear.

Even though we successfully induced hLLCs, future studies will be required to determine whether these cells can eventually fully recapitulate hLCs. One possible solution is the in vivo transplantation of hLLCs into animals, in which the microenvironment

might allow further differentiation. Beyond this, it will be of particular interest to address the survival rate and steroid secretion capability of hLLCs in vivo given the potential use of hLLC autografts in treating hypogonadism (17).

In sum, our study describes an experimental approach with the potential of providing transplantation material for clinical therapy. Moreover, hiPSC-derived LCs can potentially be used for in vitro studies of testicular development and pathologies of testis-relevant diseases and the discovery of new drugs that induce androgen formation and thus could treat hypogonadism (59).

Materials and Methods

hiPSC Maintenance and EMP Induction. The maintenance of hiPSC GM25256*B (Coriell Institute) and UCSD128i-7–5 (WiCell) and EMP induction were performed according to the manufacturers' instructions (*SI Appendix, Supplementary Methods*).

hLLC Induction. On ID 6, EMPs were passed onto 12-well plates coated with Collagen I Rat Protein solution composed of 50 g/mL Collagen I Rat Protein Solution (ThermoFisher Scientific, no. A1048301), 10× PBS, 0.417 mN NaOH, and dH_2O. Coated plates were incubated at 37 °C for at least 1 hour (h) and washed with 1× PBS 3 times. EMPs were washed with D-PBS and incubated with 1 mL of Gental Cell Dissociation Reagent (Stemcell Technologies, no. 07174) at 37 °C for 8 to 10 min. The cells were gently pipetted up and down with a 1-mL micropipette until all cells detached and then transferred into a Falcon tube containing 1 mL hLLC induction basal medium, composed of F12/DMEM, GlutaMAX, 10% FBS, and 1% P/S. The wells were washed with 2.5 mL of hLLC induction basal medium 2 times and transferred into the same tube. The collected cells were centrifuged at 300 × *g* for 7 min and resuspended in hLLC induction basal medium with 10 μM Y-27632. A total of 1 mL of medium containing 2.5×10^5 cells was plated in each well of 12-well coated plates. Cells were cultured at 37 °C for 2 d.

On ID 8, medium was changed to 900 μL of hLLC induction basal medium with 1 mM N^6,2′-O-Dibutyryladenosine 3′,5′-cyclic monophosphate (dbcAMP; Millipore Sigma, D0260) and 100 ng/mL desert hedgehog (DHH; R&D Systems, 4777-DH-050). A total of 1 μg of Steroidogenic Factor 1 (NR5A1) human-tagged ORF cloning vector (Origene, RC207577L2) was transfected into the cells using Lipofectamine 3000 and Opti-MEM according to the manufacturer's instruction. pLenti-C-mGFP–tagged cloning vector (Origene, PS100071) was used as the GFP-transfected negative control. On ID 10 and 12, medium was changed to 1 mL of fresh hLLC induction basal medium with dbcAMP and DHH.

From ID 14 to 22, cells were cultured with hLLC induction basal medium with dbcAMP, DHH, plus 150 ng/mL human chorionic gonadotropin (hCG; NIDDK, no. AFP84556A). Medium was changed every 2 d. On ID 22, cells were induced into hLLCs. *SI Appendix, Supplementary Materials and Methods* includes descriptions of qRT-PCR, ELISA analyses, immunocytochemistry, and TEM.

hALC Induction. On ID 6, EMPs were washed with D-PBS and incubated with 1 mL of Gentle Cell Dissociation Reagent at 37 °C for 8 to 10 min. The cells were gently pipetted up and down by a 1-mL micropipette until all cells detached and then transferred into a Falcon tube containing 1 mL of MesenCult-ACF Medium. The wells were washed with 2.5 mL of MesenCult-ACF Medium 2 times and transferred into the same tube. Collected cells were centrifuged at 300 × *g* for 7 min and resuspended in MesenCult-ACF Medium with 10 μM Y-27632. A total of 3 mL of medium containing 1×10^5 cells were plated into each well of 6-well MesenCult-ACF Attachment Substrate-coated plates. Cells were cultured at 37 °C with a daily half-medium change.

On ID 10, EMPs were washed with D-PBS and incubated with 1 mL of ACF Enzymatic Dissociation Solution (Stemcell Technologies, no. 05426) at 37 °C for 5 to 7 min. The reaction was stopped by 1 mL of ACF Enzyme Inhibition Solution. Cells were detached by tapping the plate. The wells were washed with 2 mL of MesenCult-ACF Medium. If more than 20% of cells remained attached, a scraper was used to detach cells. Collected cells were centrifuged at 300 × *g* for 8 min and resuspended in MesenCult-ACF Medium. A total of 1 mL of medium containing 1×10^5 cells was plated into each well of 12-well MesenCult-ACF Attachment Substrate-coated plates. Cells were cultured at 37 °C for 2 d.

On ID 12, similar to that of hLLC induction, 1 μg of NR5A1 vector or PLenti-C-mGFP–tagged vector were transfected into the cells using Lipofectamine Stem Transfection Reagent (ThermoFisher Scientific) and Opti-MEM according to the manufacturer's instruction. On ID 14 and 16, medium was changed to 1 mL of fresh MesenCult-ACF Medium with dbcAMP and DHH. From ID 18 to 24, cells were cultured with MesenCult-ACF Medium with dbcAMP, DHH, and hCG. The medium was changed every 2 d. On ID 26, cells were induced into hALCs.

Microarray Processing and Data Analyses. RNA samples were prepared using an Ambion RiboPure Kit, and microarray detection was performed with an Affymetrix Clariom S Assay, human (ThermoFisher Scientific, no. 902926), by the Children's Hospital Los Angeles Center for Personalized Medicine. Microarray data were deposited in the Gene Expression Omnibus under accession number GSE127915 (https://www.ncbi.nlm.nih.gov/geo/query/acc.cgi?acc=GSE127915; to access the data, enter token ajepmwuwnpytbif into the box). Raw CEL files were imported into the Partek Genomics Suite, and probe-level data were summarized using the RMA. Backgrounds were adjusted using RMA background correction. Quantile normalization was used to correct for array bias. All probe-level intensities were log 2-transformed. Probe sets were summarized using median polish. In total, 21,448 transcripts are represented in this array.

Gene expression data were then analyzed in the Partek Genomics Suite following the workflow for gene expression analysis to detect DE genes between samples. PCA was used to address overall similarity and differences between the samples and groups (hiPSCs, hLLCs, and hALCs). A 1-way ANOVA was used to determine which transcript had differences in expression between groups. Subsequent pairwise comparison between 2 groups was used to identify when transcripts demonstrated significant differential expression (FDR < 0.05 and fold change > 2 or < −2). Unsupervised hierarchical clustering results and heat maps were generated to identify transcripts that were specifically expressed in hiPSCs, hLLCs, or hALCs.

To identify sets of DE transcripts with biological meaning, the canonical pathways were analyzed through the use of IPA (QIAGEN). To identify the set of specifically expressed transcripts in different cell populations with steroidogenic meaning, the canonical pathways and mechanistic networks were analyzed using IPA. *SI Appendix, Supplementary Methods* includes RNA sequencing data analysis.

Western Immunoblotting. hLLCs and hiPSCs were lysed in RIPA buffer with 2% proteinase inhibitor. Human testis (NB820-59171) and adrenal whole tissue lysates (NB820-59266) were purchase from Novus Biologicals. A total of 10 μg of total proteins were resolved on 4 to 20% precast polyacrylamide gels (Bio-Rad, no. 4561096) and transferred to PVDF membranes (Millipore Sigma, ISEQ00010). After transfer, membranes were blocked with blocking solution (PBST containing 5% BSA) for 45 min and cut to allow detection of multiple antigens, guided by prestained molecular weight markers (Bio-Rad, no. 1610374). Membranes were incubated with specific primary antibodies in blocking solutions overnight at 4 °C, washed with PBST 3 times, and incubated with corresponding secondary antibodies for 1 h at RT. Then, antibodies were detected using a Clarity Western ECL Substrate system (BioRad) and visualized using an Azure c600 Western blot imaging system (Azure Biosystems, c600). Further details of membranes are provided in *SI Appendix*, Figs. S7 and S8. The use of primary antibodies and secondary antibodies is summarized in *SI Appendix, Supplementary Materials*.

Statistical Analyses. Statistical analysis was performed using GraphPad Prism 7, and statistical significance was determined using 1-way ANOVA followed by Tukey's multiple comparison test when more than 2 groups were compared. A Student's *t* test was performed when only 2 groups were compared.

ACKNOWLEDGMENTS. We thank D. Ostrow and Y. Zhu, University of Southern California (USC), for the microarray analysis; E. Daly and L. Taylor (The Research Institute of the McGill University Health Centre) for assistance with liquid chromatography with tandem mass spectrometry studies; and A. Rodriguez (Doheny Eye Institute, USC) for technical assistance with transmission electron microscopy. This work was supported by funds from the School of Pharmacy and the John Stauffer Dean's Chair in Pharmaceutical Sciences (USC).

1. L. Li, K. K. Miu, S. Gu, H. H. Cheung, W. Y. Chan, Comparison of multi-lineage differentiation of hiPSCs reveals novel miRNAs that regulate lineage specification. *Sci. Rep.* **8**, 9630 (2018).
2. B. R. Zirkin, V. Papadopoulos, Leydig cells: Formation, function, and regulation. *Biol. Reprod.* **99**, 101–111 (2018).
3. A. H. Payne, D. B. Hales, Overview of steroidogenic enzymes in the pathway from cholesterol to active steroid hormones. *Endocr. Rev.* **25**, 947–970 (2004).
4. M. C. Beattie, L. Adekola, V. Papadopoulos, H. Chen, B. R. Zirkin, Leydig cell aging and hypogonadism. *Exp. Gerontol.* **68**, 87–91 (2015).
5. T. G. Travison, A. B. Araujo, A. B. O'Donnell, V. Kupelian, J. B. McKinlay, A population-level decline in serum testosterone levels in American men. *J. Clin. Endocrinol. Metab.* **92**, 196–202 (2007).
6. I. Huhtaniemi, G. Forti, Male late-onset hypogonadism: Pathogenesis, diagnosis and treatment. *Nat. Rev. Urol.* **8**, 335–344 (2011).

7. H. Chemes *et al*., Isolation of human Leydig cell mesenchymal precursors from patients with the androgen insensitivity syndrome: Testosterone production and response to human chorionic gonadotropin stimulation in culture. *Biol. Reprod.* **46**, 793–801 (1992).
8. J. Qin, M. J. Tsai, S. Y. Tsai, Essential roles of COUP-TFII in Leydig cell differentiation and male fertility. *PLoS One* **3**, e3285 (2008).
9. S. M. Mendis-Handagama, H. B. Ariyaratne, Differentiation of the adult Leydig cell population in the postnatal testis. *Biol. Reprod.* **65**, 660–671 (2001).
10. T. Yazawa *et al*., Differentiation of adult stem cells derived from bone marrow stroma into Leydig or adrenocortical cells. *Endocrinology* **147**, 4104–4111 (2006).
11. L. Hou *et al*., Gonadotropins facilitate potential differentiation of human bone marrow mesenchymal stem cells into Leydig cells in vitro. *Kaohsiung J. Med. Sci.* **32**, 1–9 (2016).
12. T. Tanaka *et al*., Steroidogenic factor 1/adrenal 4 binding protein transforms human bone marrow mesenchymal cells into steroidogenic cells. *J. Mol. Endocrinol.* **39**, 343–350 (2007).
13. S. Yamanaka, Induced pluripotent stem cells: Past, present, and future. *Cell Stem Cell* **10**, 678–684 (2012).
14. T. Sonoyama *et al*., Differentiation of human embryonic stem cells and human induced pluripotent stem cells into steroid-producing cells. *Endocrinology* **153**, 4336–4345 (2012).
15. B. P. Schimmer, P. C. White, Minireview: Steroidogenic factor 1: Its roles in differentiation, development, and disease. *Mol. Endocrinol.* **24**, 1322–1337 (2010).
16. X. Li *et al*., Regulation of seminiferous tubule-associated stem Leydig cells in adult rat testes. *Proc. Natl. Acad. Sci. U.S.A.* **113**, 2666–2671 (2016).
17. H. Arora *et al*., Subcutaneous leydig stem cell autograft: A promising strategy to increase serum testosterone. *Stem Cells Transl. Med.* **8**, 58–65 (2019).
18. T. Yazawa, Y. Imamichi, K. Miyamoto, A. Umezawa, T. Taniguchi, Differentiation of mesenchymal stem cells into gonad and adrenal steroidogenic cells. *World J. Stem Cells* **6**, 203–212 (2014).
19. A. Uezumi, T. Kasai, K. Tsuchida, Identification, isolation, and characterization of mesenchymal progenitors in mouse and human skeletal muscle. *Methods Mol. Biol.* **1460**, 241–253 (2016).
20. A. Uezumi *et al*., Identification and characterization of PDGFRα+ mesenchymal progenitors in human skeletal muscle. *Cell Death Dis.* **5**, e1186 (2014).
21. K. J. Teerds, I. T. Huhtaniemi, Morphological and functional maturation of Leydig cells: From rodent models to primates. *Hum. Reprod. Update* **21**, 310–328 (2015).
22. M. A. Wood *et al*., Fetal adrenal capsular cells serve as progenitor cells for steroidogenic and stromal adrenocortical cell lineages in M. musculus. *Development* **140**, 4522–4532 (2013).
23. X. Xing *et al*., Differentiation of human umbilical cord mesenchymal stem cells into steroidogenic cells *in vitro*. *Exp. Ther. Med.* **12**, 3527–3534 (2016).
24. H. H. Yao, W. Whoriskey, B. Capel, Desert Hedgehog/Patched 1 signaling specifies fetal Leydig cell fate in testis organogenesis. *Genes Dev.* **16**, 1433–1440 (2002).
25. A. Antoniou-Tsigkos, E. Zapanti, L. Ghizzoni, G. Mastorakos, "Adrenal androgens" in *Endotext*, K. R. Feingold *et al*., Eds. (MDText.com, South Dartmouth, MA, 2000).
26. Y. Nakamura *et al*., Type 5 17beta-hydroxysteroid dehydrogenase (AKR1C3) contributes to testosterone production in the adrenal reticularis. *J. Clin. Endocrinol. Metab.* **94**, 2192–2198 (2009).
27. J. Paranko, Expression of type I and III collagen during morphogenesis of fetal rat testis and ovary. *Anat. Rec.* **219**, 91–101 (1987).
28. W. L. Miller, H. S. Bose, Early steps in steroidogenesis: Intracellular cholesterol trafficking. *J. Lipid Res.* **52**, 2111–2135 (2011).
29. L. Issop, M. B. Rone, V. Papadopoulos, Organelle plasticity and interactions in cholesterol transport and steroid biosynthesis. *Mol. Cell. Endocrinol.* **371**, 34–46 (2013).
30. B. Jégou, S. Sankararaman, A. D. Rolland, D. Reich, F. Chalmel, Meiotic genes are enriched in regions of reduced archaic ancestry. *Mol. Biol. Evol.* **34**, 1974–1980 (2017).
31. Y. Shima *et al*., Contribution of Leydig and Sertoli cells to testosterone production in mouse fetal testes. *Mol. Endocrinol.* **27**, 63–73 (2013).
32. M. Inoue *et al*., Isolation and characterization of fetal leydig progenitor cells of male mice. *Endocrinology* **157**, 1222–1233 (2016).
33. F. Arakane *et al*., The mechanism of action of steroidogenic acute regulatory protein (StAR). StAR acts on the outside of mitochondria to stimulate steroidogenesis. *J. Biol. Chem.* **273**, 16339–16345 (1998).
34. A. M. Courtot *et al*., Morphological analysis of human induced pluripotent stem cells during induced differentiation and reverse programming. *Biores. Open Access* **3**, 206–216 (2014).
35. A. H. Payne, M. P. Hardy, L. D. Russell, *The Leydig Cell* (Cache River Press, Vienna, IL, 1996).
36. A. K. Christensen "Leydig cells" in *Handbook of* Physiology*, Section 7,* Vol. *5, Male* Reproductive System. D. W. Hamilton, R. D. Greep, eds (American Physiological Society, Washington, DC, 1975), pp 57–94.
37. H. Chemes, "Leydig cell development in humans" in *The Leydig Cell* (Cache River Press, Vienna, IL, 1996), pp. 175–202.
38. F. P. Prince, Mitochondrial cristae diversity in human Leydig cells: A revised look at cristae morphology in these steroid-producing cells. *Anat. Rec.* **254**, 534–541 (1999).
39. C. D. Folmes *et al*., Somatic oxidative bioenergetics transitions into pluripotency-dependent glycolysis to facilitate nuclear reprogramming. *Cell Metab.* **14**, 264–271 (2011).
40. S. Oka, K. Shiraishi, H. Matsuyama, Effects of human chorionic gonadotropin on testicular interstitial tissues in men with non-obstructive azoospermia. *Andrology* **5**, 232–239 (2017).
41. T. C. Hsieh, A. W. Pastuszak, K. Hwang, L. I. Lipshultz, Concomitant intramuscular human chorionic gonadotropin preserves spermatogenesis in men undergoing testosterone replacement therapy. *J. Urol.* **189**, 647–650 (2013).
42. G. P. Risbridger, D. M. Robertson, D. M. de Kretser, The effects of chronic human chorionic gonadotropin treatment on Leydig cell function. *Endocrinology* **110**, 138–145 (1982).
43. F. Arakane *et al*., Phosphorylation of steroidogenic acute regulatory protein (StAR) modulates its steroidogenic activity. *J. Biol. Chem.* **272**, 32656–32662 (1997).
44. P. R. Manna, S. P. Chandrala, Y. Jo, D. M. Stocco, cAMP-independent signaling regulates steroidogenesis in mouse Leydig cells in the absence of StAR phosphorylation. *J. Mol. Endocrinol.* **37**, 81–95 (2006).
45. D. M. Stocco, X. Wang, Y. Jo, P. R. Manna, Multiple signaling pathways regulating steroidogenesis and steroidogenic acute regulatory protein expression: More complicated than we thought. *Mol. Endocrinol.* **19**, 2647–2659 (2005).
46. P. R. Manna *et al*., Regulation of steroidogenesis and the steroidogenic acute regulatory protein by a member of the cAMP response-element binding protein family. *Mol. Endocrinol.* **16**, 184–199 (2002).
47. Z. C. Johnston *et al*., The human fetal adrenal produces cortisol but no detectable aldosterone throughout the second trimester. *BMC Med.* **16**, 23 (2018).
48. M. Goto *et al*., In humans, early cortisol biosynthesis provides a mechanism to safeguard female sexual development. *J. Clin. Invest.* **116**, 953–960 (2006).
49. E. Chamoux, L. Bolduc, J. G. Lehoux, N. Gallo-Payet, Identification of extracellular matrix components and their integrin receptors in the human fetal adrenal gland. *J. Clin. Endocrinol. Metab.* **86**, 2090–2098 (2001).
50. S. Y. Park, M. Tong, J. L. Jameson, Distinct roles for steroidogenic factor 1 and desert hedgehog pathways in fetal and adult Leydig cell development. *Endocrinology* **148**, 3704–3710 (2007).
51. M. Chen *et al*., Wt1 is involved in leydig cell steroid hormone biosynthesis by regulating paracrine factor expression in mice. *Biol. Reprod.* **90**, 71 (2014).
52. B. Troppmann, G. Kleinau, G. Krause, J. Gromoll, Structural and functional plasticity of the luteinizing hormone/choriogonadotrophin receptor. *Hum. Reprod. Update* **19**, 583–602 (2013).
53. G. Ruiz-Babot *et al*., Modeling congenital adrenal hyperplasia and testing interventions for adrenal insufficiency using donor-specific reprogrammed cells. *Cell Rep.* **22**, 1236–1249 (2018).
54. A. Midzak, V. Papadopoulos, Adrenal mitochondria and steroidogenesis: From individual proteins to functional protein assemblies. *Front. Endocrinol. (Lausanne)* **7**, 106 (2016).
55. D. H. Margineantu, D. M. Hockenbery, Mitochondrial functions in stem cells. *Curr. Opin. Genet. Dev.* **38**, 110–117 (2016).
56. F. P. Prince, Ultrastructural evidence of mature Leydig cells and Leydig cell regression in the neonatal human testis. *Anat. Rec.* **228**, 405–417 (1990).
57. W. J. Shen, S. Azhar, F. B. Kraemer, Lipid droplets and steroidogenic cells. *Exp. Cell Res.* **340**, 209–214 (2016).
58. L. Russel, S. Burguet, Ultrastructure of leydig cells as revealed by secondary tissue treatment with a ferrocyanide-osmium mixture. *Tissue Cell* **9**, 751–766 (1977).
59. M. S. Elitt, L. Barbar, P. J. Tesar, Drug screening for human genetic diseases using iPSC models. *Hum. Mol. Genet.* **27**, R89–R98 (2018).